

Blurring of Light due to Multiple Scattering by Participating Medium: A Path Integral Approach

Michael Ashikhmin

Simon Premože

Ravi Ramamoorthi

Shree Nayar

CUCS-017-04

Department of Computer Science
Columbia University
450 Computer Science Building
1214 Amsterdam Avenue
New York, NY 10027

May 31, 2004

Abstract

Volumetric light transport effects are significant for many materials like skin, smoke, clouds or water. In particular, one must consider the multiple scattering of light within the volume. Recently, we presented a path integral-based approach to this problem which identifies the most probable path light takes in the medium and approximates energy transport over all paths by only those surrounding this most probable one. In this report we use the same approach to derive useful expressions for the amount of spacial and angular blurring light experiences as it travels through a medium.

Blurring of Light due to Multiple Scattering by Participating Medium: A Path Integral Approach

Michael Ashikhmin¹ Simon Premože² Ravi Ramamoorthi¹
Shree Nayar¹

May 31, 2004

Abstract

Volumetric light transport effects are significant for many materials like skin, smoke, clouds or water. In particular, one must consider the multiple scattering of light within the volume. Recently, we presented a path integral-based approach to this problem which identifies the most probable path light takes in the medium and approximates energy transport over all paths by only those surrounding this most probable one. In this report we use the same approach to derive useful expressions for the amount of spacial and angular blurring light experiences as it travels through a medium.

1 Introduction

Volumetric scattering effects are important for making realistic computer graphics images of many materials like skin, fruits, milk, clouds, and smoke. In these cases, we cannot make the common assumption that light propagates without scattering in straight lines. Indeed, the *multiple scattering* of light in participating media is important for many qualitative effects [4, 3] like glows around light sources in foggy weather, or subsurface scattering in human skin, or the spreading of a beam in a scattering medium.

Light transport, including multiple scattering in arbitrary scattering media, can be accurately computed by solving the radiative transfer equation [5, 8], the volumetric analogue to the rendering equation. Volumetric

Monte Carlo and finite element techniques (volumetric ray tracing and radiosity) have been used by many researchers in the past [17, 11, 12, 2, 14, 9]. However, volumetric multiple scattering effects are notoriously difficult to simulate, even using the best Monte Carlo approaches, taking hours to days. For this reason, these effects are not usually present in computer graphics imagery, and certainly not in interactive systems. Thus, one must look for simpler approximations and analytic models.

While it is possible to simulate such media using volumetric Monte Carlo or finite element techniques, those methods are very computationally expensive. On the other hand, simple analytic models have so far been limited to homogeneous and/or optically dense media and cannot be easily extended to include strongly directional effects and visibility in spatially varying volumes. We would like to develop a simple practical approach for efficiently simulating volumetric effects in general spatially varying inhomogeneous scattering media, taking directionally-varying lighting effects into account. We choose an approach based on path integration framework [18] to achieve this goal. The initial development was presented [16] but the resulting algorithm remained rather complicated and we would like to have something more practical. We describe resulting algorithms the complete system elsewhere [15]. This report concentrates on deriving the key expression for spacial width used by our system. It also contains a derivation of analogous expression for angular blurring which can be useful for future extensions of our approach. These developments are presented in sections 5 and 6, respectively. Prior to this, we present necessary preliminaries and a short outline of the path integral approach. Readers familiar with the subject and especially with our related work [16, 15] can go directly to section 5.

2 Effects of Multiple Scattering

If we shine a laser beam pulse into a scattering media, the pulse undergoes a series of absorption and scattering events. The effects of multiple scattering result in significant changes to the pulse illustrated by Figure 1:

1. **Spatial spreading** The pulse cross-section broadens as it propagates through media. We incorporate this effect into our algorithm presented in [15]

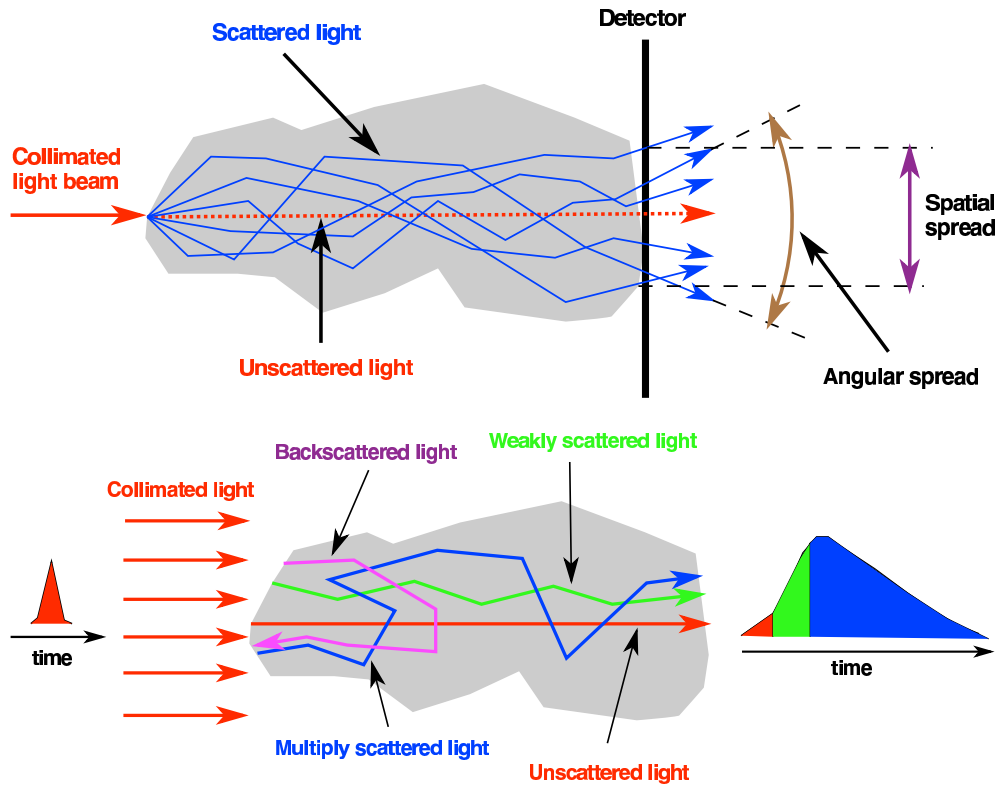


Figure 1: Beam spreading in scattering media due to multiple scattering.

2. **Angular spreading** The angular divergence of a narrow pulse gets larger as it travels through the medium. We do not currently incorporate such effects into the algorithm but provide necessary mathematical results for doing so with a procedure similar to that used for spatial blurring.
3. **Temporal spreading** Scattered photons of the pulse stay behind the original unscattered photons since they have to take longer paths. The direct consequence is that pulse becomes longer as it travels through the medium. While this effect is very important in many fields such as remote sensing [22], it is of little interest for computer graphics which deals with stationary solutions of light transport. We will, however, see that explicit treatment of time (or distance) dependence is very useful as an intermediate step.

a	Absorption coefficient
b	Scattering coefficient
c	Extinction coefficient ($a + b$)
g	Mean cosine of scattering angle
s	variable corresponding to time
x	offset from MPP
A	Action
G	Green's propagator
L	Radiance
P	Phase function
Q	Source
S	Original path length of Most Probable Path (MPP)
$\langle\theta^2\rangle$	Mean square scattering angle
α	$1/4(1 - g) = 1/(2\langle\theta^2\rangle)$
ξ	Vector of parameters corresponding to path
w	Spatial width of paths

Table 1: Selected symbols

Many of the subtle appearance effects of scattering materials are a direct consequence of beam spreading due to multiple scattering. As we see, it is straightforward to qualitatively understand beam spreading and stretching in the scattering media, but direct simulation of multiple scattering and therefore of spreading (blurring) is computationally expensive. The quantitative analysis of spatial and angular spreading we present could provide more insight into appearance of scattering materials and could lead to more efficient and simpler rendering algorithms.

3 Mathematical Preliminaries

In this section, we introduce the mathematical preliminaries of the radiative transfer equation and path integration as the necessary background for our derivations in the following sections.

3.1 Radiative Transfer Equation

Optical properties of volumetric materials can be characterized by density $\rho(\mathbf{x})$, their scattering and absorption coefficients $b(\mathbf{x})$ and $a(\mathbf{x})$, the extinction

coefficient $c(\mathbf{x}) = a(\mathbf{x}) + b(\mathbf{x})$, and the phase function $P(\mathbf{x}, \vec{\omega}, \vec{\omega}')$. The phase function P describes the probability of light coming from incident direction $\vec{\omega}$ scattering into direction $\vec{\omega}'$ at point \mathbf{x} . The phase function is normalized, $\int_{4\pi} P(\vec{\omega}, \vec{\omega}') d\omega' = 1$ and only depends on the phase angle $\cos \theta = \vec{\omega} \cdot \vec{\omega}'$. The mean cosine g of the scattering angle is defined as

$$g = \int_{4\pi} P(\vec{\omega}, \vec{\omega}') (\vec{\omega} \cdot \vec{\omega}') d\omega'.$$

and the average square of the scattering angle $\langle \theta^2 \rangle$ is

$$\langle \theta^2 \rangle = 2\pi \int_0^\pi \theta^2 P(\vec{\omega}, \vec{\omega}') \sin \theta d\theta. \quad (1)$$

The value of g qualitatively describes the properties of the medium. If $g = 0$, the medium is isotropic (constant phase function), while a forward scattering medium like clouds or mist will have g positive. The phase function as defined here only describes what happens when light is scattered by a single particle. It has no recollection about which direction the particle was redirected to before. The phase function P is independent from what happened in previous scattering events and it is unimportant when light gets absorbed.

The most general case of light transport in arbitrary media is described by the time-dependent radiative transport equation [5, 8],

$$\left(\frac{\partial}{\partial s} + \vec{\omega} \cdot \nabla + c(\mathbf{x}) \right) L(s, \mathbf{x}, \vec{\omega}) = b(\mathbf{x}) \int_{4\pi} d\Omega' P(\vec{\omega}, \vec{\omega}') L(s, \mathbf{x}, \vec{\omega}') + Q(s, \mathbf{x}, \vec{\omega}), \quad (2)$$

where we have expressed time t in units of length s , with $s = vt$. As compared to the standard time-independent equation, we have introduced the term $\partial/\partial s$ on the left-hand side. $Q(s, \mathbf{x}, \vec{\omega})$ is the source term, accounting for emitted illumination from light sources.

From the general theory of linear integral equations [1], it is known that the solution of equation 2 can be expressed as a convolution of the initial source radiance distribution $Q = L_0(\mathbf{x}', \vec{\omega}')$ with a Green's function or propagator (evolution operator) $G(s, \mathbf{x}, \mathbf{x}', \vec{\omega}, \vec{\omega}')$:

$$L(s, \mathbf{x}, \vec{\omega}) = \int G(s, \mathbf{x}, \mathbf{x}', \vec{\omega}, \vec{\omega}') L_0(\mathbf{x}', \vec{\omega}') d\mathbf{x}' d\vec{\omega}'. \quad (3)$$

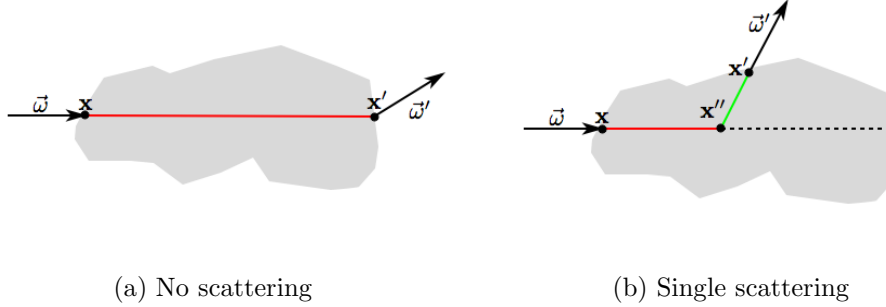


Figure 2: Green’s propagator for the light transport equation can be related to marching along a ray and computing effects of attenuation operator $G_{noscatter}$ and single-scattering operator G_{single} .

Physically, the Green propagator $G(s, \mathbf{x}, \mathbf{x}', \vec{\omega}, \vec{\omega}')$ represents radiance at point \mathbf{x} in direction $\vec{\omega}$ at time s due to light emitted at time zero by a point light source located at \mathbf{x}' shining in direction $\vec{\omega}'$. Mathematically, it is the solution of the homogeneous version of equation 2 (i.e. with source term set to zero) with initial condition expressed using the Dirac delta function δ as

$$G(s = 0, \mathbf{x}, \vec{\omega}, \mathbf{x}', \vec{\omega}') = \delta(\mathbf{x} - \mathbf{x}')\delta(\vec{\omega} - \vec{\omega}'). \quad (4)$$

3.2 Green’s propagator and relation to raytracing

In the absence of scattering ($b = 0$), the solution for the complete propagator G is almost trivial:

$$G(s, \mathbf{x}, \vec{\omega}, \mathbf{x}', \vec{\omega}') \equiv G_{noscatter}(s, \mathbf{x}, \vec{\omega}, \mathbf{x}', \vec{\omega}') = \quad (5)$$

$$\delta(\mathbf{x} - \vec{\omega}s - \mathbf{x}')\delta(\vec{\omega} - \vec{\omega}') \times \exp\left\{-\int_0^s c(\mathbf{x} - \vec{\omega}(s - s'))ds'\right\}. \quad (6)$$

Here the light travels in a straight line and is attenuated by the absorption coefficient $a(\mathbf{x}) = c(\mathbf{x})$. One can see that in this case, the formulation using the propagator is equivalent to simple raytracing (Figure 2). This simple attenuation model is quite popular in computer graphics and it is often part of popular APIs like OpenGL (fog attenuation).

We can also write the propagator G to include an arbitrary number of scattering events. For example, single scattering propagator G_{single} includes

light that has been scattered only once and the light that has not been scattered at all (as above). To formalize it, we note that propagation from starting position and direction $(x', \vec{\omega}')$ to final position and direction $(x, \vec{\omega})$ requires three steps. First, light is attenuated over distance s' to an intermediate point \mathbf{x}'' . Second, the light scatters at point \mathbf{x}'' from initial direction $\vec{\omega}'$ to final direction $\vec{\omega}$. Only a fraction that is determined by the phase function P of the incident radiance scatters into the new direction. Third, light is further attenuated from the intermediate point \mathbf{x}'' to the final point \mathbf{x}' . To include all possible intermediate points where a scattering event occurs, the propagator G_{single} is given by integration over all intermediate points:

$$G_{single}(s, \mathbf{x}, \vec{\omega}, \mathbf{x}', \vec{\omega}') = G_{noscatter}(s, \mathbf{x}, \vec{\omega}, \mathbf{x}', \vec{\omega}') + \quad (7)$$

$$\int_0^s ds' \int_{|\mathbf{x}'' - \mathbf{x}'| = s'} \int_{S^2} \{G_{noscatter}(s - s', \mathbf{x}, \vec{\omega}, \mathbf{x}'', \vec{\omega}''') \times b(\mathbf{x}'')$$

$$\int_{S^2} P(\mathbf{x}'', \vec{\omega}'', \vec{\omega}''') G_{noscatter}(s', \mathbf{x}'', \vec{\omega}'', \mathbf{x}', \vec{\omega}') d\omega''\} d\omega''' dx''.$$

This expression again directly corresponds to the standard single scattering ray marching algorithm commonly used in computer graphics. Marching along the viewing ray and sending shadow rays (that are also attenuated) toward a light source corresponds to the three steps discussed above (Figure 2).

We could further rewrite the propagator to include higher order of scattering events by recursively expanding the propagator. But, as demonstrated by equation 7, the expression would quickly become unmanageably complex due to additional angular integrations that have to be performed to account for higher orders of scattering. Therefore, it is often useful in practice to split the propagator G into two parts: unscattered and single-scattered (or “direct”) light $G_d = G_{single}$ and one for multiply scattered (or “indirect”) light G_s and solve them separately:

$$G(s, \mathbf{x}, \vec{\omega}, \mathbf{x}', \vec{\omega}') = G_d(s, \mathbf{x}, \vec{\omega}, \mathbf{x}', \vec{\omega}') + G_s(s, \mathbf{x}, \vec{\omega}, \mathbf{x}', \vec{\omega}') \quad (8)$$

The initial condition for the scattered light propagator G_s is straightforward, because there is no multiply scattered light in the beginning:

$$G_s(s = 0, \mathbf{x}, \vec{\omega}, \mathbf{x}', \vec{\omega}') = 0 \quad (9)$$

We will use existing techniques for computing direct lighting described by G_d . Our main goal in this work will be to efficiently deal with the propagator G_s (multiply-scattered light) that could lead to faster rendering algorithms for participating media.

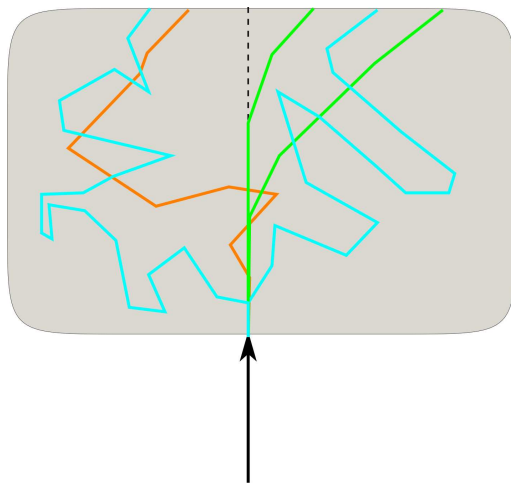


Figure 3: There are infinitely many paths by which the light can reach the eye through a scattering media, and the total visible luminance is the sum over all such paths. However, some paths (cyan) clearly contribute very little to the final image. Furthermore, some paths (green) are more probable than others (red) given optical properties of the medium even if they are otherwise comparable.

3.3 Path Integral Formulation

The path integral (PI) approach provides a particular way to express the propagator $G(s, \mathbf{x}, \vec{\omega}, \mathbf{x}', \vec{\omega}')$. It is based on the simple observation that the full process of energy transfer from one point to another can be thought of as a sum over transfer events taking place along many different paths connecting points \mathbf{x} and \mathbf{x}' , each subject to boundary conditions restricting path directions at these points to $\vec{\omega}$ and $\vec{\omega}'$, respectively (see Figure 3). The full propagator is then just an integral of individual path contributions over all such paths. This object is called the *path integral*. One can further notice that the intensity of light travelling along each path will be only diminishing due to absorption and scattering events along the path. This is because in-scattering into the path, which is generally treated as a process increasing light intensity, in a particular direction will be due to photons travelling a *different* path in the medium (we ignore here exact backscattering which can return photons exactly to the same path). Therefore, if we introduce effective attenuation τ along the path, we can write the individual path contribution

(weight) as $\exp(-\tau)$, and the complete propagator as

$$G \sim \int \exp(-\tau(\text{path})) \mathcal{D}x, \quad (10)$$

where the attenuation τ is analogous to the classical *action* A along the path, with $\exp(-\tau(\text{path})) \sim \exp(-A(\text{path}))$.

Because the integration is performed over the infinite-dimensional path space using highly non-intuitive differential measure $\mathcal{D}x$ defined for it, the mathematics of path integrals is exceptionally complex [6, 10]. Tessendorf [19] derived a path integral expression for the propagator G in homogeneous materials. Interested readers are referred to his further work [20, 21] for detailed derivations of the path integral formulation. Using much simpler tools, one can still obtain some useful results [16] of the PI theory, which we will present here without detailed derivations.

First, part of path weight or action due to multiple scattering in the integral in equation 10 can be shown to be proportional to:

$$\exp\left(-\int_0^s \left[a(\vec{\gamma}_P(s')) + \frac{\alpha}{b(\vec{\gamma}_P(s'))} \left| \frac{d\theta}{ds'} \right|^2 \right] ds' \right), \quad (11)$$

where $\vec{\gamma}(s)$ is a pathlength parameterized path, $d\theta/ds$ is its curvature, and $\alpha = 1/4(1 - g) = 1/(2\langle\theta^2\rangle)$, where $\langle\theta^2\rangle$ is the mean square scattering angle. Integration is performed along the path.

One can find a path which maximizes this expression (i.e. has minimal attenuation or action among all possible paths). We call it the most probable path (MPP). For the important special case of homogeneous media under boundary conditions when path directions are specified at both ends, one can determine the shape of MPP of given length analytically with the standard Euler-Lagrange minimization procedure [7]. The result is a “uniformly turning” path of constant curvature which is changing its direction at a constant rate.

We further assume that only a small fraction of paths “around” the MPP contribute significantly to the integral and will restrict the integral to account for the contribution of these important paths only. Formally, this constitutes a Wentzel-Kramer-Brillouin (WKB) expansion [10] of the path integral while physically and visually it accounts for the fact that blurring of the luminance

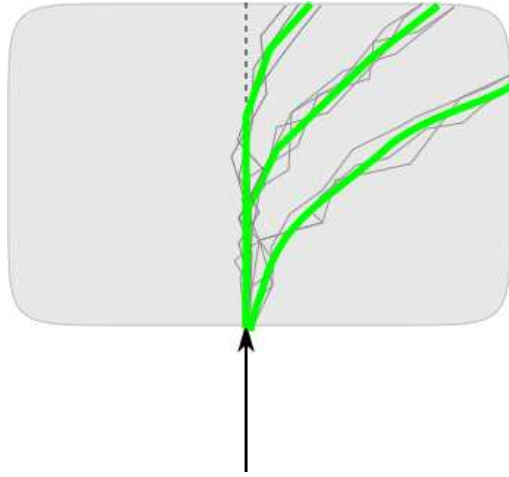


Figure 4: Once we find a set of most probable paths for given initial conditions, we compute contributions along those paths and some neighborhood around these paths. All other paths are ignored because they are deemed not important. In practice, we do not even consider the full set of MPPs, but rather a subset of those which are the easiest to treat.

distribution is the most notable characteristic of participating media. The basic idea of our approach, using the most probable path, and a neighborhood around it, is shown in Figure 4.

4 Surrounding Path Contribution

In computer graphics, a boundary condition of particular interest is a *single-sided* one, which requires the path to start at a particular point in space with particular initial direction (an example is the eye position and primary viewing ray direction) but applies no additional restrictions on the second end of the path. The path will usually terminate once it reaches an object (or a light source) in the scene. Suppose we found the MPP for this boundary condition and computed its contribution. We would now like to approximate the complete path integral by taking into account only the contribution of “surrounding” paths. This operation formally constitutes a WKB expansion of the integral.

If we parameterize the family of nearby paths using some vector of parameters $\vec{\xi}$ (with $\vec{\xi}=0$ at the MPP), the path integral can be written as an

integral over these parameters. Note that because A in equation 11 has the global minimum at the MPP, its expansion in terms of parameters $\vec{\xi}$ will start from square terms. That is, if there is only one parameter ξ , a simple Taylor series is,

$$A(\xi) = A(0) + \frac{1}{2}\xi^2 \frac{\partial^2 A}{\partial \xi^2} + \dots,$$

$$\exp(-A(\text{path})) \sim \exp(-A(\text{MPP})) \exp\left(-\frac{1}{2}\xi^2 \frac{\partial^2 A}{\partial \xi^2}\right) \quad (12)$$

where the linear term in the top equation is omitted because $A(0)$ is a minimum, and $A(0)$ corresponds to the action for the most probable path. Note that the bottom equation has a gaussian form, giving weights to nearby paths according to their “distance” from the MPP. If $\vec{\xi}$ is now a vector, we may write the propagator in equation 10 as

$$G \sim \exp(-A(\text{MPP})) \int_{\xi} \exp(-(\xi \nabla_{\xi})^2 A/2) d\xi. \quad (13)$$

The first term here is the MPP contribution and the integral is over re-parameterized path space. Although integration space is still infinite-dimensional, we can use this expression to estimate some important properties of the radiance distribution by writing out the expansion of A for some family of nearby paths in terms of relevant parameters while keeping others fixed. In particular, we will be interested in radiation blurring along the path, which can be measured by the *spatial width* of contributing paths, as shown in Figure 5.

5 Estimation of Spatial Blur

For the purposes of blurring size estimation, we can assume without loss of generality that the MPP is a straight line ¹. We are also interested for now only in spatial, and not angular blurring (which will be considered next). Thus, we consider only paths with the same incident and outgoing directions, as shown in Figure 5. For a path displaced from the straight line MPP by a distance x , we consider a path consisting of two circular segments stitched together, as shown on the right of Figure 5. Paths of this family both fulfill boundary conditions, including the new one of path end direction coinciding

¹A space warp can be performed to bring a curved path to this case.

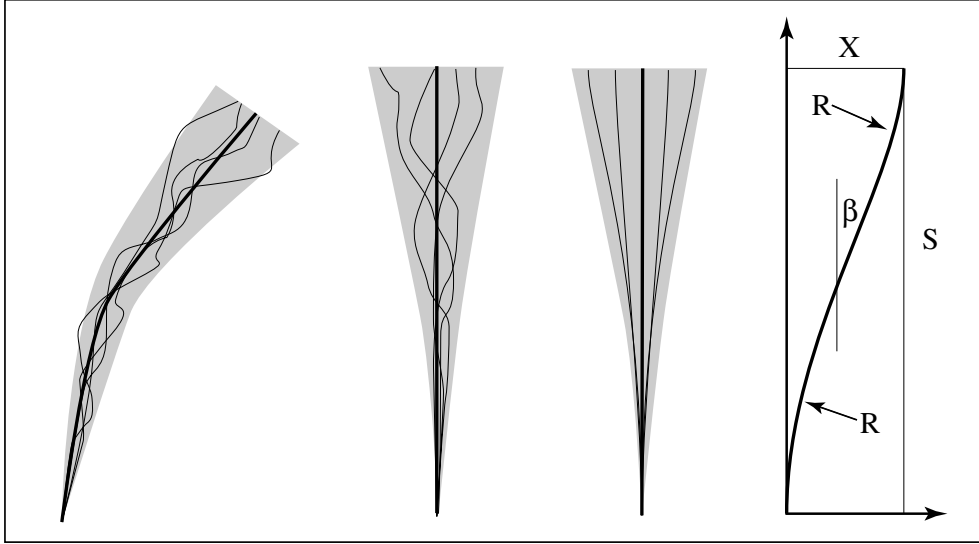


Figure 5: A sequence of simplifications for the paths considered. Contributions are Gaussian with respect to both space and path end direction. Only the first factor is considered by applying an extra boundary condition. Left to right: original MPP (thick) and nearby paths; straightened MPP and paths contributing to spatial blurring; special family of double circle paths which is being treated exactly; parameters for a double circle path. The region of nearby path concentration is shown in grey.

with that of MPP (necessary to exclude blurring in the space of directions) and are expected to be effective energy transporters due to their uniformly low curvature and low additional length compared to the MPP. We will compute analytically the width of the path distribution in this family for homogeneous media, and assume that the result gives a reasonable estimation for the total spatial blurring.

We can rewrite A for such paths, shown in Figure 5, and integrate over each of the circular segments separately per equation 11,

$$A(x) = 2 \int_0^s \left(a + \frac{\alpha}{bR^2} \right) ds', \quad (14)$$

where the curvature is given by $1/R$ and R is the circle radius. Now, we

switch variables to the turning angle β , since $ds' = R d\beta$,

$$A(x) = 2 \int_0^{\beta_{max}} \left(aR + \frac{\alpha}{bR} \right) d\beta = 2 \left(aR + \frac{\alpha}{bR} \right) \beta_{max}. \quad (15)$$

For the end point offset x , simple geometric computations give $R = (S^2 + x^2)/4x$ and the maximum turning angle $\beta_{max} = \arcsin(S/2R) \approx 2x/S - 2x^3/3S^3$ where S is the original path length and we have performed Taylor expansion in small parameter x/S . Substituting these values into equation 15 and performing further Taylor series expansion, we get:

$$\begin{aligned} 2 \left(aR + \frac{\alpha}{bR} \right) \beta_{max} &= \left(\frac{a(S^2 + x^2)}{4x} + \frac{4\alpha x}{b(S^2 + x^2)} \right) \left(\frac{4x}{S} - \frac{4x^3}{3S^3} \right) \\ &= aS + x^2 \left(\frac{a}{S} - \frac{a}{3S} + \frac{16\alpha}{bS(S^2 + x^2)} \right) + \dots \\ &\approx A(0) + x^2 \left(\frac{2a}{3S} + \frac{16\alpha}{bS^3} \right) \end{aligned} \quad (16)$$

As expected from the form of equation 12, this expansion starts from quadratic terms in x . This will allow us to write the width of the Gaussian distribution of paths in this family as

$$w^2 = \frac{1}{2} \left(\frac{2a}{3S} + \frac{16\alpha}{bS^3} \right)^{-1} = \frac{\langle \theta^2 \rangle b S^3}{16(1 + S^2/12l^2)}, \quad (17)$$

which we will use as an estimation of the overall blurring along the path in our rendering algorithm. Here we introduced “diffusive path length” $l^2 = 1/(ab\langle \theta^2 \rangle)$.

Limiting Cases. For long paths ($S \gg l$), the square of the spatial width grows linearly along the path (with S): $w^2 = \frac{3}{4}\langle \theta^2 \rangle b S l^2$. For another special case of no absorption ($l = \infty$) $w^2 = b\langle \theta^2 \rangle S^3/16$. For these limiting cases, using much more rigorous derivation Tessendorf [18] obtained the spatial width of $w^2 = b\langle \theta^2 \rangle S^3/24$ for case with no absorption and $w^2 = b\langle \theta^2 \rangle l^2 S$ with absorption. We obtain a correct functional dependence on both S and medium parameters, but are off by a constant factor of 3/2 in comparison to Tessendorf. We offset this discrepancy by introducing a constant 2/3 correction factor to our expression.

Being relatively simple, our approach provides a single easy to evaluate expression for spacial blurring. When a comparison with much more sophisticated theoretical methods is possible, the accuracy of our expression seems

sufficient given the needs of computer graphics applications giving more solid ground to our results. Note also that more rigorous approaches typically do not provide a general closed form solution at all and only special cases similar to those present above can be evaluated. McLean[13] discusses beam spread functions in more depth and provides a comparison between different analytic models.

6 Angular blur strength estimation

In this section we present a simple treatment of angular blurring due to multiple scattering. Although we do not currently use these results in our implementation, corresponding algorithm which would treat non-directional light sources more accurately can be designed based on the approach presented in [15].

We will follow the general procedure outlined in section 5 to estimate the strength of angular blurring along the path. We will again make the same simplifying approximations to arrive at an analytic solution, namely, we will assume that MPP is a straight line, the medium is homogeneous and deviation of sufficiently significant surrounding paths from MPP is small enough to allow Taylor expansion in relevant parameters. We will also need a new modified boundary condition to isolate angular blurring. We will therefore consider only paths starting and ending at the same positions as MPP and furthermore, only those which have the same starting direction as the MPP. Among these paths we will now select a set of paths which we expect to be effective light transporters while still allowing a closed form treatment. We choose the one parameter family of asymmetric double-circular-segment paths of the type shown on Figure 6. We can uniquely specify a particular path by its final deviation angle ϕ . For such paths we can express action A from equation 11 as

$$A(x) = 2 \int_0^{\beta_{max}} \left(aR + \frac{\alpha}{bR} \right) d\beta + \int_0^{\phi} \left(aR + \frac{\alpha}{bR} \right) d\beta \quad (18)$$

Note that the first term is the same as the one we considered for the problem of spacial blurring and we know the result for this part already. However, it is not very useful since it is not expressed in terms of final deviation ϕ . Instead, since curvature radius is constant for the paths we chose and arclength is just $ds = Rd\beta$, we re-write equation 18 as an integral over path length to arrive

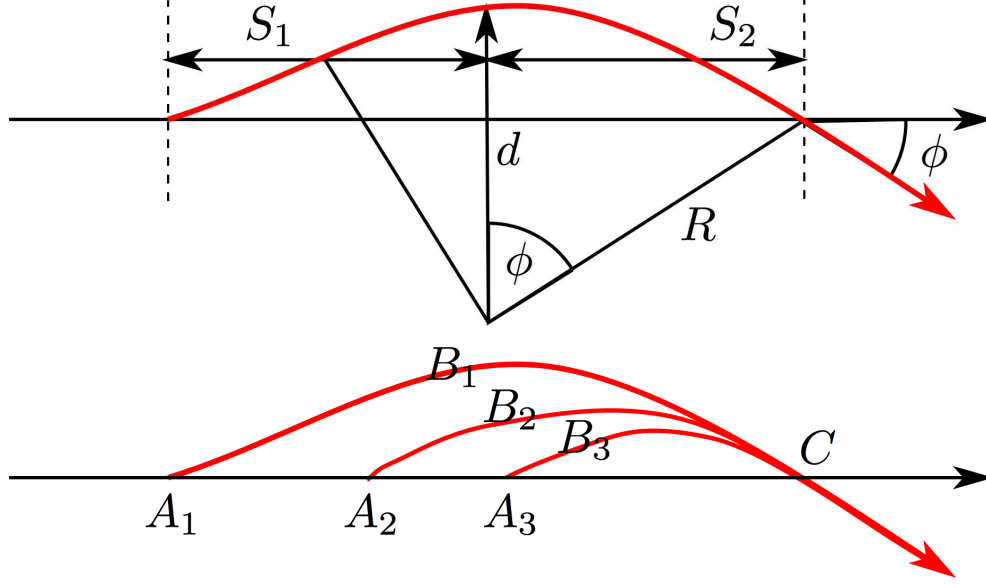


Figure 6: Top: Geometry of the path used for angular blurring width derivation. Bottom: Blurring width is a non-decreasing quantity. Paths with shorter curved part are more efficient energy transporters and while blurring width decreases with S for paths of A_1B_1C type, it can not be less than the maximum width reached in the family shown.

at

$$A(x) = \left(as + \frac{\alpha}{bR^2}s \right) \quad (19)$$

where s is the total length of the curved double circular path which we have to express through MPP length S and deviation angle ϕ . We now split the MPP into two parts by the point corresponding to maximum spatial deviation d . We then have $S = R\sin\phi + 2\sqrt{R^2 - (R - d/2)^2}$. d in turn can be expressed as $d = R - R\cos\phi$. We can now compute radius R of the circle as $R = S/(\sin\phi + \sqrt{3 - 2\cos\phi - \cos^2\phi}) \approx S/((1 + \sqrt{2})\phi)$. This immediately gives approximate expression for the curvature-related second part of equation 19 as $\phi^2\alpha(1 + \sqrt{2})^2/(bS)$. The total length of the path can be computed using standard approximate expressions for the length of a circular sector: $l = \sqrt{S_1^2 + 16/3(d/2)^2} + (1/2)\sqrt{(2S_2)^2 + 16/3d^2}$ and length difference from the MPP is $\Delta s = l - (S_1 + S_2) \approx 2d^2/3(1/S_1 + 1/S_2)$. Substituting expressions for lengths of two parts of the MPP $S_2 = R\sin\phi$, $S_1 = S - S_2$ and then for the circle radius, we obtain $\Delta s = (2/3)R^2(1 - \cos\phi)^2(1/(R\sin\phi) + 1/(S - R\sin\phi)) =$

$(2/3)S(1 - \cos\phi)^2/(\sin\phi\sqrt{3 - 2\cos\phi - \cos^2\phi}) \approx S\phi^2/(6\sqrt{2})$. Substituting this result into the expression for A , we finally get expansion around the MPP which, as expected, starts from second order terms in ϕ :

$$A(x) = A(0) + \left(\frac{aS}{6\sqrt{2}} + \frac{\alpha(1 + \sqrt{2})^2}{bS} \right) \phi^2 \quad (20)$$

Gaussian angular blurring radius is then

$$w_a^2 = \frac{1}{2} \left(\frac{aS}{6\sqrt{2}} + \frac{\alpha(1 + \sqrt{2})^2}{bS} \right)^{-1} = \frac{3\sqrt{2}bS}{abS^2 + 6\sqrt{2}\alpha(1 + \sqrt{2})^2} \quad (21)$$

For short paths ($S \ll l$, $l^2 = 1/(ab\langle\theta^2\rangle)$) or cases with no absorption ($a = 0$) this expression gives $w_a^2 = (1/(1 + \sqrt{2})^2)b\langle\theta^2\rangle S \approx (1/5.8)b\langle\theta^2\rangle S$ where we used the expression for α . Generally accepted result of rigorous treatment for this case gives $w_a^2 = (1/3)b\langle\theta^2\rangle S$ which is a very reasonable agreement given the simplicity of our approach.

However, for the other limiting case of long paths ($S \gg l$) we obtain a non-physical result of blurring radius *decreasing* with distance and need to examine this case more closely. We note that paths which follow MPP exactly for some fraction of their length, as shown on the bottom of Figure 6 for paths A_2B_2C and A_3B_3C , are even more efficient light transporters as the “fully curved” paths A_1B_1C we considered. We can write analytic expression for blurring due to such path in a way similar to equation 21 with adjusted length S' . We then see that a more accurate expression for blurring radius will be

$$w_a = \max_{all A} (w_a(path ABC)) = \max_{0 < S' < S} w_a(S') \quad (22)$$

As long as w_a grows with S , maximum value is achieved for $S' = S$ and equation 21 can be used directly as we did for short path/no absorption case. In general, we need to find the point S_{max} where w_a expression has the maximum and, if path is long enough to contain this point, use $w_a(S_{max})$. This immediately means that for long paths blurring angle will reach a constant value (rather than decreasing). Taking the derivative of equation 21 and performing substitution, we obtain $w_a^2(S \gg l) = 2\sqrt{3\sqrt{2}}/(1 + \sqrt{2})\langle\theta^2\rangle bl \approx 1.7\langle\theta^2\rangle bl$ Rigorous treatment in this case also predicts constant blurring radius which is expressed as $w_a^2 = \langle\theta^2\rangle bl$.

7 Conclusion

In this report we derived expressions for spatial and angular blurring of light due to multiple scattering in a medium using path integral formulation. We would like to emphasize again that we presented here an hugely simplified treatment of the problem and never expected to get an exact answer. It is therefore quite encouraging to see that we were able to obtain *in all cases where more rigorous results are available* correct functional dependence of both spatial and angular blurring radiuses on *all* relevant parameters. The fact that all constants in our estimations of blurring radius are always within a factor of two from corresponding accurate results is even more remarkable. We hope that both the results themselves and simple procedures used in their derivation will be useful in developing efficient rendering algorithms for multiply scattering participating media. We presented a version of such algorithm in [15].

8 Acknowledgements

We would like to thank Jerry Tessendorf for helpful discussions of path integral formulation. This work was supported in part by grants from the National Science Foundation (CCF #0305322 on Real-Time Visualization and Rendering of Complex Scenes) and Intel Corporation (Real-Time Interaction and Rendering with Complex Illumination and Materials).

References

- [1] G. I. Bell and S. Glasstone. *Nuclear Reactor Theory*. Van Nostrand Reinhold, New York, 1970.
- [2] P. Blasi, B. Le Saec, and C. Schlick. A rendering algorithm for discrete volume density objects. *Computer Graphics Forum*, 12(3):201–210, 1993.
- [3] Craig F. Bohren. *Clouds in a glass of beer*. John Wiley and Sons, 1987.
- [4] Craig F. Bohren. Multiple scattering of light and some of its observable consequences. *American Journal of Physics*, 55(6):524–533, June 1987.
- [5] S. Chandrasekar. *Radiative Transfer*. Dover, New York, 1960.

- [6] R. P. Feynman and A. R. Hibbs. *Quantum mechanics and path integrals*. McGraw-Hill Higher Education, 1965.
- [7] Charles Fox. *An Introduction to the Calculus of Variations*. Dover, New York, 1987.
- [8] A. Ishimaru. *Wave Propagation and Scattering in Random Media. Volume 1: Single Scattering and Transport Theory*. Academic Press, 1978.
- [9] Henrik Wann Jensen and Per H. Christensen. Efficient simulation of light transport in scenes with participating media using photon maps. In *Proceedings of SIGGRAPH 98*, Computer Graphics Proceedings, Annual Conference Series, pages 311–320, Orlando, Florida, July 1998.
- [10] Flor Langouche, Dirk Roekaerts, and Enrique Tirapegui. *Functional Integration and Semiclassical Expansions*. D. Reidel Publishing Company, 1982.
- [11] E. Languenou, K. Bouatouch, and M. Chelle. Global illumination in presence of participation media with general properties. In *Eurographics Rendering Workshop*, pages 69–85, 1994.
- [12] N. Max. Efficient light propagation for multiple anisotropic volume scattering. In *Eurographics Rendering Workshop*, pages 87–104, 1994.
- [13] John W. McLean, Jonathan D. Freeman, and Ronald E. Walker. Beam spread function with time dispersion. *Applied Optics-LP*, 37(21):4701–4711, July 1998.
- [14] S. Pattanaik and S. Mudur. Computation of global illumination in a participating medium by monte carlo simulation. *Journal of Visualization and Computer Animation*, 4(3):133–152, 1993.
- [15] Simon Premože, Michael Ashikhmin, Ravi Ramamoorthi, and Shree Nayar. Rendering of multiple scattering effects in participating media. In *Eurographics Symposium on Rendering*, 2004.
- [16] Simon Premože, Michael Ashikhmin, and Peter Shirley. Path integration for light transport in volumetric materials. In *Proceedings of the Eurographics Symposium on Rendering*, 2003.
- [17] H. Rushmeier and K. Torrance. The zonal method for calculating light intensities in the presence of a participating medium. In *SIGGRAPH 87*, pages 293–302, 1987.

- [18] Jerry Tessororf. Radiative transfer as a sum over paths. *Phys. Rev. A*, 35:872–878, 1987.
- [19] Jerry Tessororf. Time-dependent radiative transfer and pulse evolution. *J. Opt. Soc. Am. A*, (6):280–297, 1989.
- [20] Jerry Tessororf. The Underwater Solar Light Field: Analytical Model from a WKB Evaluation. In Richard W. Spinrad, editor, *SPIE Underwater Imaging, Photography, and Visibility*, volume 1537, pages 10–20, 1991.
- [21] Jerry Tessororf. Measures of temporal pulse stretching. In Gary D. Gilbert, editor, *SPIE Ocean Optics XI*, volume 1750, pages 407–418, 1992.
- [22] Ronald E. Walker and John W. McLean. Lidar equations for turbid media with pulse stretching. *Applied Optics*, 38(12):2384–2397, April 1999.